C. R. Geoscience 350 (2018) 55–64

Contents lists available at ScienceDirect

Comptes Rendus Geoscience

www.sciencedirect.com

Hydrology, Hydrogeology

Dynamics of floodplain lakes in the Upper Amazon Basin during the late Holocene

Isabel Quintana-Cobo [a,*], Patricia Moreira-Turcq [a], Renato C. Cordeiro [b], Keila Aniceto [b], Alain Crave [c], Pascal Fraizy [a], Luciane S. Moreira [b], Julia Maria de Aguiar Duarte Contrera [b], Bruno Turcq [d]

[a] IRD (Institut de recherche pour le développement), GET (Geosciences Environnement Toulouse), UMR 5563, Toulouse, France
[b] Departamento de Geoquimica, Universidade Federal Fluminense (UFF), Niteroi, Brazil
[c] Géosciences Rennes, UMR 6118, Université de Rennes-1, Rennes, France
[d] IRD-Sorbonne Universités (UPMC, Univ Paris 06)-CNRS-MNHN, LOCEAN Laboratory, Universidad Peruana Cayetano Heredia, Lima, Peru

ARTICLE INFO

Article history:
Received 23 June 2016
Accepted after revision 10 October 2017
Available online 9 January 2018

Handled by François Chabaux

Keywords:
Upper Amazon Basin
Late Holocene
Abrupt accumulation events
Lake sedimentation

ABSTRACT

To better understand the impact of channel migration processes and climate change on the depositional dynamics of floodplain lakes of the upper Amazon Basin during the late Holocene, we collected three sediment cores from floodplain lakes of the Ucayali River and one from the Marañón River. The cores were dated with ^{14}C, radiographed and described. Bulk density, grain size analysis and total organic carbon (TOC) were determined. The results show that sedimentation in Ucayali floodplain lakes was marked by variations during the late Holocene, with periods of intense hydrodynamic energy and abrupt accumulations, a gap in the record between about 2870 and 690 cal yr BP, and periods of more lacustrine conditions. These changes in sedimentation were associated with variations in the river's influence related to changes in its meandering course (2870 cal yr BP) and a period of severe flooding between 3550 and 3000 cal yr BP. Lake Lagarto on the Marañón River floodplain exhibits a different sedimentary environment of low hydrodynamics with palm trees and macrophytes. Apparently, the lake has not experienced intense migration processes during the last 600 cal yr BP (base of the core). Nevertheless, the river sediment flux to the lake was important from 600 to 500 cal yr BP, although it decreased thereafter until the present. This decrease in the mineral accumulation rate indicates a decrease in river discharge since 500 cal yr BP, which coincides with precipitation records from the central Andes. In the upper part of the three Ucayali floodplain cores, a 30- to 250-cm-thick layer of reworked sediments has been deposited since 1950 AD (post-bomb). In Lake Carmen, this layer is associated with invasion of the lake by the levee of a migrating meander of the Ucayali. In Lakes Hubos and La Moringa, however, the river is still far away and the deposition must be interpreted as the result of extreme flooding. The beginning of the Ucayali meander migration is dated back to 2000 AD, suggesting that these extreme floods could be very recent and linked to hydrologic extremes registered instrumentally in the Amazon Basin.

* Corresponding author.
E-mail address: isabel.amazona.quintana3@gmail.com (I. Quintana-Cobo).

https://doi.org/10.1016/j.crte.2017.10.004
1631-0713/

1. Introduction

The main source of sediment in the Amazon River and its major tributaries is Andean erosion (Filizola and Guyot, 2009; Filizola et al., 2011; Gibbs, 1967; Martinez et al., 2009; Meade et al., 1979). Most of the rivers originating in the Andes Mountains present a high-suspended load (80%) and low bed load (20%) (Meade et al., 1985). During transport from the Andes to the Atlantic Ocean, sediments are exposed to many processes: sedimentation, temporary storage, resuspension and reworking (Dunne et al., 1998; Moreira-Turcq et al., 2014; Santini et al., 2014). It indicates that this transport through lowland Amazonia involves sediment exchanges between the channel and the floodplain. These exchanges occur through bank erosion, bar deposition, and overbank sedimentation in floodplain (Irion et al., 2006; Moreira-Turcq et al., 2014). Sediment dynamics are complex, and floodplain deposits have been reworked and incorporated into Amazonian streams. The estimated rates of recycling are less than 5000 yr in the case of the modern floodplain of the downstream Óbidos in lower Amazon Basin and 2000 cal yr BP upstream (Mertes et al., 1996).

The lowland Amazon Basin shows a relatively immobile channel, unlike the strongly active migration processes and sedimentary dynamics in the upper Amazon (Quintana, 2015). Floodplains in the upper Amazon Basin are impacted by channel migrations that can be triggered by flood events (Jerolmack and Mohrig, 2007), sediment loads (Constantine et al., 2014) or drainage network segmentation induced by tectonic activity (Costa et al., 2001). Past fluvial dynamics are not well documented in this region. In general, channel lateral migration is related to Holocene neotectonics, which suggests that the shifting of rivers may be caused by either tilting of the basin surface or subsidence of blocks in the basin basement (Dumont, 1996; Dumont and Fournier, 1994; Franzinelli and Igreja, 2002; Latrubesse and Franzinelli, 2002; Räsänen et al., 1990). However, hydrological changes are also important, Constantine et al. (2014) suggested that rivers with high sediment loads experience annual migration rates greater than those of rivers with lower sediment loads. Meander cut-off occurred more frequently along rivers with higher sediment loads, and the authors concluded that the imposed sediment loads influenced the changes in fluvial processes in the lower Amazon Basin. Nevertheless, Quintana (2015) points out the importance of temporal and spatial scales to study fluvial dynamics. Finally, all these studies show that sediment deposition in Amazonia floodplain lakes is not constant over time and can be influenced strongly by several factors. Understanding how paleoclimatic changes and geomorphological processes can affect sedimentation in the Amazonian floodplain lakes remains a challenge.

The main purpose of this work is to understand and determine the main processes responsible for lacustrine deposition in floodplain lakes of the upper Amazon Basin during the late Holocene. For this, was collected four sedimentary cores in floodplain lakes from the Ucayali and Marañon meandering rivers, which present different characteristics in terms of sediment load, sinuosity and water flux.

2. Material and methods

2.1. Study area

The Amazon River drains the largest basin of the planet, with an estimated area of 6.1×10^6 km^2 (Goulding et al., 2003) and is formed at the confluence of the Ucayali and Marañón Rivers in Peruvian Amazonia (Fig. 1A). The Ucayali River drains the southern part of the Peruvian Andean Cordillera and flows into the Marañón River, draining 360,000 km^2, with a mean annual discharge of approximately 11,200 m^3·s^{-1}. The Marañón River drains 350,000 km^2 from the northern and central parts of the Peruvian Andean Cordillera to its confluence with the Ucayali, with a mean annual discharge of 16,200 m^3·s^{-1} (Espinoza-Villar et al., 2012).

The suspended sediment load varies according to the season. The annual average concentration of suspended sediment is 395 mg·L^{-1} at the Requena station (Ucayali River) and 173 mg·L^{-1} at the San Regis station (Marañón River) (Armijos et al., 2013). The width of the Ucayali River varies from 500 m to 1250 m. The average sinuosity is 1.94, the belt meandering current is 30 km wide and is characterized by multiple abandoned channels (Dumont, 1996). The width of the Marañón River varies from 1000 to 2500 m, with numerous islands in the straight sections. The average sinuosity is 1.33. The Marañón's flow is 14% greater than that of the Ucayali River. Average annual rainfall between 1946 and 1994 was of about 3080 mm·yr^{-1} (Marengo et al., 1998). Precipitation is most intense between January and May. The hydrological cycle is very similar in the Marañón and Ucayali rivers, with flood peaks occurring between March and May, and low waters between August and October.

The study area is in Peruvian Amazonia, in the department of Loreto between 5°00'S–74°40'W and 4°00'S–73°20'W (Fig. 1B). This study analysed three lakes in the Ucayali River floodplain: Lakes Hubos and La Moringa (Fig. 1C1), Lake Carmen (Fig. 1C2), and one lake in the Marañón River floodplain, Lake Lagarto (Fig. 1C3), which is located 200 km from the confluence with the Ucayali River.

2.2. Sampling and analyses

Four cores were collected in the upper Amazon Basin (Fig. 1). The CAR2 (4°35'23"S and 73°28'.45"W) and HUB1 (4°30'29.19"S and 73°23'.40"W) cores were collected in Lakes Carmen and Hubos using a "vibro-core." The MOR1 (4°28'48.61"S and 73°24'11.04"W) and LAG1 (4°31'04.81"S and 74°34'55.15"W) cores were collected manually in Lakes La Moringa and Lagarto, respectively. All cores were collected using aluminium tubes 7.5 cm in diameter. The CAR2, HUB1, MOR1 and LAG1 cores (measuring 600, 140, 120 and 98 cm, respectively) were opened, described and analysed with SCOPIX X-ray equipment at the EPOC ("Environnements et paléoenvi-

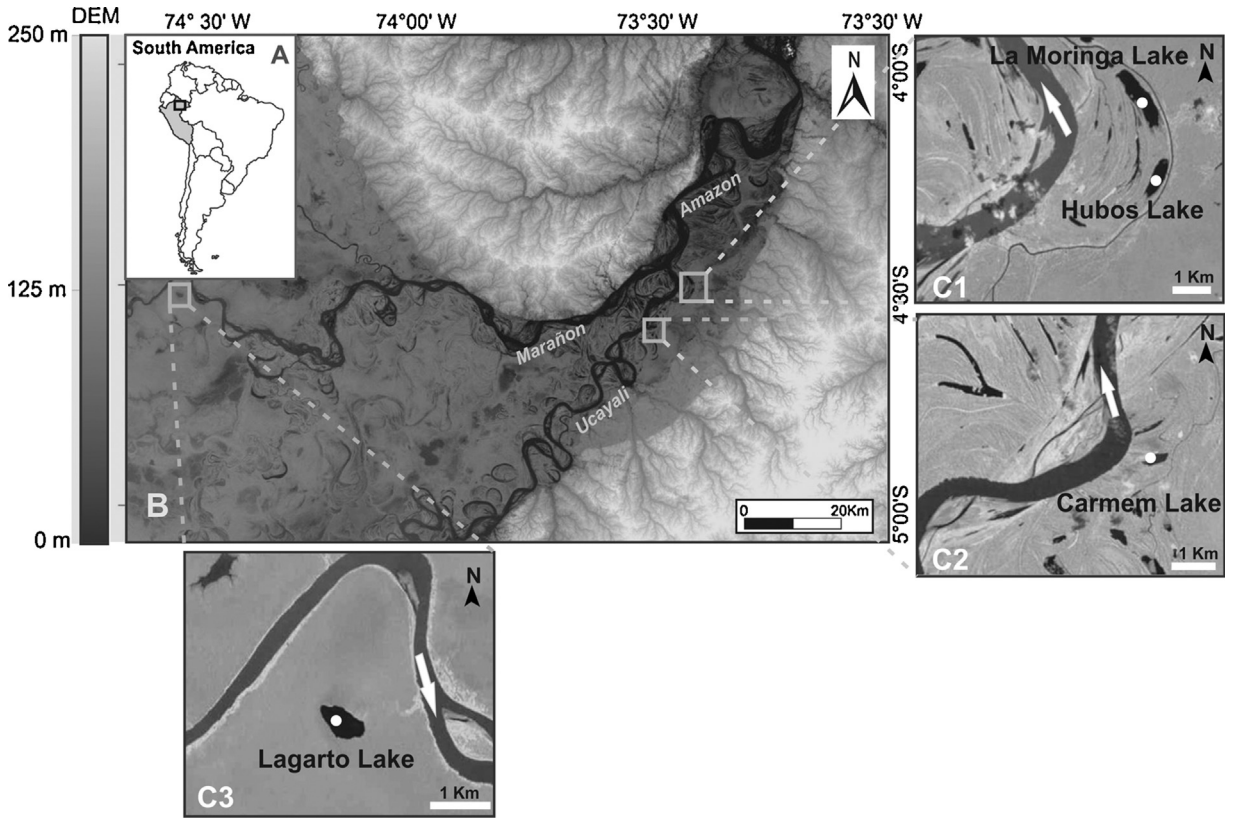

Fig. 1. Location of the confluence of the Ucayali and Marañón Rivers. A, Peru location. B, DEM of the study area. C1, Lakes La Moringa and Hubos. C2, Lake Carmen. C3, Lake Lagarto in the Marañón floodplain.

ronnements océaniques et continentaux") laboratory at the University of Bordeaux-1 (France). Scopix uses classical X-ray equipment (X-ray source: 160 kV, 19 mA), coupled with new radioscopy instrumentation (CCD camera 756 Å ~ 581 resolution), connected to a computer for data acquisition and processing (Migeon et al., 1998).

2.2.1. Water content and bulk density

Soon after opening, the sediment was sampled in aluminium U-channels to determine sediment bulk density and water content. Sub-samples were taken every 1 cm along the cores, and the water content was measured after oven drying at 40 °C for several days to obtain a final stable weight.

2.2.2. Radiocarbon dating

^{14}C measurements were performed with an Artemis accelerator mass spectrometry (AMS) system based on a 3-MV Pelletron from National Electrostatics Corporation (NEC, Middleton, Wisconsin, USA) at the "Laboratoire de mesure du carbone 14" (LMC14) — UMS 2572 (CEA/DSM CNRS IRD IRSN—"Ministère de la Culture et de la Communication"). The age–depth model was built using CLAM (non-Bayesian code 'classical' age-depth models). CLAM is written in the open-source R statistical environment and allows calibration of ^{14}C dates, building an age model based on decisions made by the user, and producing graphs and text files (Blaauw, 2010). The four cores were dated, and the age models use the IntCal 13 ^{14}C calibration curve and a polynomial regression. Calibrated ages are expressed in conventional cal yr BP.

2.2.3. Particle size analysis

A laser particle size analyser (CILAS 1064) was used to measure the grain-size distribution. Samples were treated with hydrogen peroxide to remove organic matter, and a sodium hexametaphosphate ($Na_{16}P_{14}O_{43}$) solution (40 mg·L^{-1}) was used to assist in dispersing the particles.

2.2.4. Elemental carbon composition

Total organic carbon (TOC) composition was determined with a CHN analyser (FISIONS NA-2000) at the University of California, Davis, CA, USA. Samples were first treated with 0.5 N HCl to remove carbonates.

2.2.5. Digital Elevation Model (DEM)

Free Landsat-5 sensor/TM images were acquired through the INPE ("Instituto Nacional de Pesquisas Espaciais") website (http://www.dgi.inpe.br/CDSR/), using the 006/063 scene. Free SRTM (Shuttle Radar Topography Mission) data were available on the US Geological Survey website (http://www.gdex.cr.usgs.gov/gdex/), with a resolution of 30 m. Data were processed using Global Mapper 13 software, where different colour levels were assigned to highlight the different dimensions of the region and to

evidence morphological and topographical features (Fig. 1B).

3. Results

3.1. Chronology and lithology

Eighteen samples along the CAR2 core were dated and presented an older age of 4612 cal yr BP (Table 1). Eight radiocarbon dates were obtained from the HUB1 core, with an age of 3215 cal yr BP for the basal section (Table 1). Twelve TOC AMS radiocarbon dates were obtained for the MOR1 core, with an age of 2961 cal yrs BP (Table 1). In the MOR1 and CAR2 cores collected in the Ucayali floodplain, the age model (Fig. 2) was based on a cubic-spline curve to the calibrated ^{14}C ages and in the HUB1 core, the age model was based on a polynomial regression. A gap in sedimentation records was observed in the three sediment cores. This gap is well dated in the HUB1 record and occurs between 2950 and 719 cal yr BP. A sediment package of remobilized sediment, likely due to reworking of older sediment, occurred at the top of the three cores and was not considered in the age model. Four TOC AMS dates defined the sedimentary chronology of the LAG1 core, with a basal age of 630 cal yr BP and a probably modern top age (Fig. 2). No upper package of reworked sediment is observed in this core.

The CAR2, MOR1 and HUB1 cores are comprised of sediments that are poor in organic matter, with a predominance of silt and sand in the CAR2 core and silt and clay in the MOR1 and HUB1 cores (Fig. 3). Nevertheless, low carbon content, organic-rich layers containing plant remains can be identified along the three cores. These layers can be observed:

- in the CAR2 core between 449–420 cm and 76–56 cm;
- in the MOR1 core between 81–64 cm, 45–32 cm and 20–0 cm;
- in the HUB1 at 45–44 cm.

The LAG1 core is composed of organic-rich clay with plant remains.

Table 1
Radiocarbon and calibrated dates of the LAG1, CAR2, HUB1 and MOR1 core samples.

Core	Lab. Number	Depth (cm)	Radiocarbon age	Calibrated age (cal BP)	cal BP ages (2 sigma)
LAG1 (Maranon)	SacA 24998	0–1	110 ± 30	115	12–269
	SacA 24999	29–30	310 ± 30	400	301–463
	SacA 25000	62–63	445 ± 30	607	465–534
	SacA 25001	97–98	605 ± 30	630	545–653
CAR2 (Ucayali)	Beta 319436	0–1	Post-modern	Post-1955	–
	SacA 29547	38–39	2105 ± 30	2077	1997–2148
	SacA 29548	61–62	1385 ± 30	1302	1275–1344
	SacA 29549	78–79	840 ± 30	747	686–796
	SacA 29550	102–103	2345 ± 30	2354	2320–2443
	SacA 29551	160–161	1740 ± 30	1653	1566–1713
	SacA 29552	220–221	2670 ± 30	2775	2748–2809
	SacA 29553	253–254	Post-modern	Post-1955	–
	SacA 29554	261–262	Post-modern	Post-1955	–
	Beta 319438	268–269	170 ± 30	180	133–228
	SacA 29555	280–281	600 ± 30	604	542–653
	SacA 29556	330–331	2050 ± 30	1995	1932–2072
	SacA 29557	390–391	3315 ± 30	3535	3459–3614
	Beta 319439	410–411	3640 ± 30	3952	3869–4005
	SacA 29558	474–475	3320 ± 30	3545	3475–3632
	SacA 29559	534–535	3555 ± 30	3840	3723–3960
	Beta 319440	574–575	4120 ± 30	4620	4528–4815
	SacA 29560	578–579	4100 ± 30	4612	4452–4811
HUB1 (Ucayali)	SacA 26760	2–3	1535 ± 30	1489	1358–1522
	SacA 26761	33–34	Post-modern	Post-1955	–
	SacA 26762	40–41	Post-modern	Post-1955	–
	SacA 26763	44–45	Post-modern	Post-1955	–
	SacA 26764	80–81	Post-modern	Post-1955	–
	SacA 26765	117–118	810	719	681–770
	SacA 26766	121–122	2840 ± 30	2950	2886–3037
	Beta 305452	139–140	3020	3215	3140–3271
MOR1 (Ucayali)	SacA 25002	0.5–1.5	1330 ± 30	1275	1184–1208
	SacA 25003	13–14	860 ± 30	765	694–800
	SacA 25004	19–20	Post-modern	Post-1955	–
	SacA 25005	22–23	Post-modern	Post-1955	–
	SacA 25006	30–31	335 ± 30	390	309–476
	SacA 25007	45–46	320 ± 30	388	305–466
	SacA25008	53–54	1045 ± 30	954	921–1000
	SacA 25009	70.5–71.5	940 ± 30	905	792–924
	SacA 25010	80–81	670 ± 30	660	559–676
	SacA 25011	94–95	1160 ± 30	1070	983–1176
	SacA 25012	107–108	2535 ± 30	2724	2494–2746
	SacA 25013	115–116	2850 ± 30	2961	2876–3059

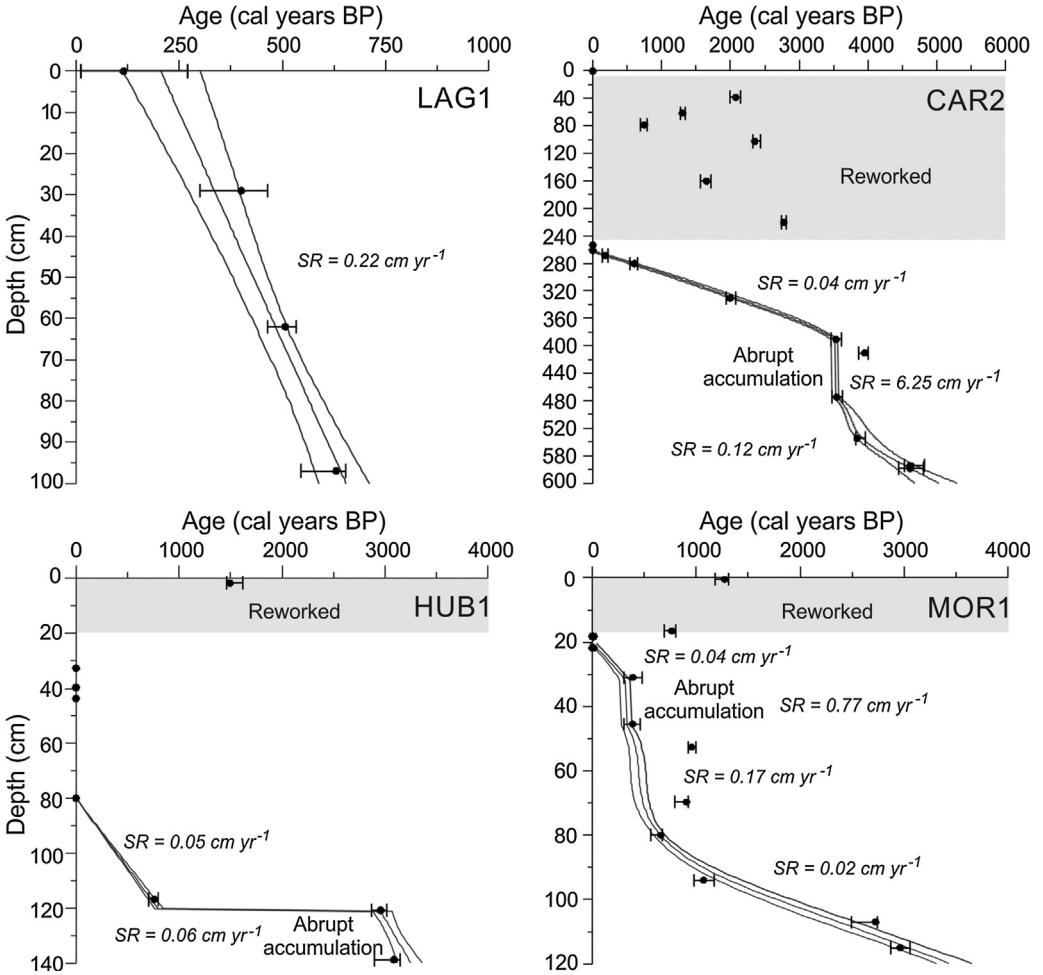

Fig. 2. The chronological age models for the four studied cores.

3.2. Bulk density

The sedimentary bulk density in the CAR2, HUB1 and MOR1 cores averages was 1.01 g·cm^{-3}, 0.78 g·cm^{-3} and 0.73 g·cm^{-3}, respectively, ranging from 0.31 g·cm^{-3} to 1.65 g·cm^{-3}, 0.40 g·cm^{-3} to 1.53 g·cm^{-3} and 0.39 to 1.26 g·cm^{-3}, respectively (Fig. 3). The LAG1 core presented lower bulk density values than the Ucayali cores, with an average of 0.19 g·cm^{-3}, ranging from 0.05 g·cm^{-3} to 0.45 g·cm^{-3} (Fig. 3).

3.3. Grain-size fractions

The sediment grain size analysis of the CAR2 core was characterized by a predominance of coarser sediments. Mean values for clay and fine silt are 3% and 20%, respectively, with values for medium silt, coarser silt, and fine sand of 19%, 40% and 18%, respectively (Fig. 3). Analysis of the MOR1 and HUB1 cores showed predominance of clay and fine silt. The mean percentages of clay, fine silt, medium silt and coarse silt, were 33%, 51%, 15% and 1% in MOR1 and 32%, 46%, 17% and 5% in HUB1, without traces of sand (Fig. 3). In the LAG1 core, a predominance of clay and fine silt can be observed, with mean values of 53% and 42%, respectively, and with low values for medium silt, with an average of 5% (Fig. 3).

3.4. Total Organic Carbon

The carbon content of the CAR2 core averaged 1.01 wt%, ranging from 0.25 wt% to 11.7 wt%, with a significant increase between 256 cm and 288 cm (Fig. 3). The HUB1 core had relatively low TOC levels, between 0.56 wt% and 5.38 wt%, with an average of 1.94 wt% (Fig. 3). The MOR1 core had also low TOC levels, between 1.09 and 5.4 wt%, with a mean content of 2.40 wt% (Fig. 3). The LAG1 core TOC values were very high, with mean values of 25.7 wt%, ranging from 8.06 wt% to 50 wt% (Fig. 3).

4. Discussion

4.1. Recent fluvial dynamics of the Ucayali and Marañón Rivers

The Ucayali, Marañón and Beni Rivers are responsible for nearly all of the sediments transported by the Amazon (Guyot et al., 2007). More than 540 million tons of

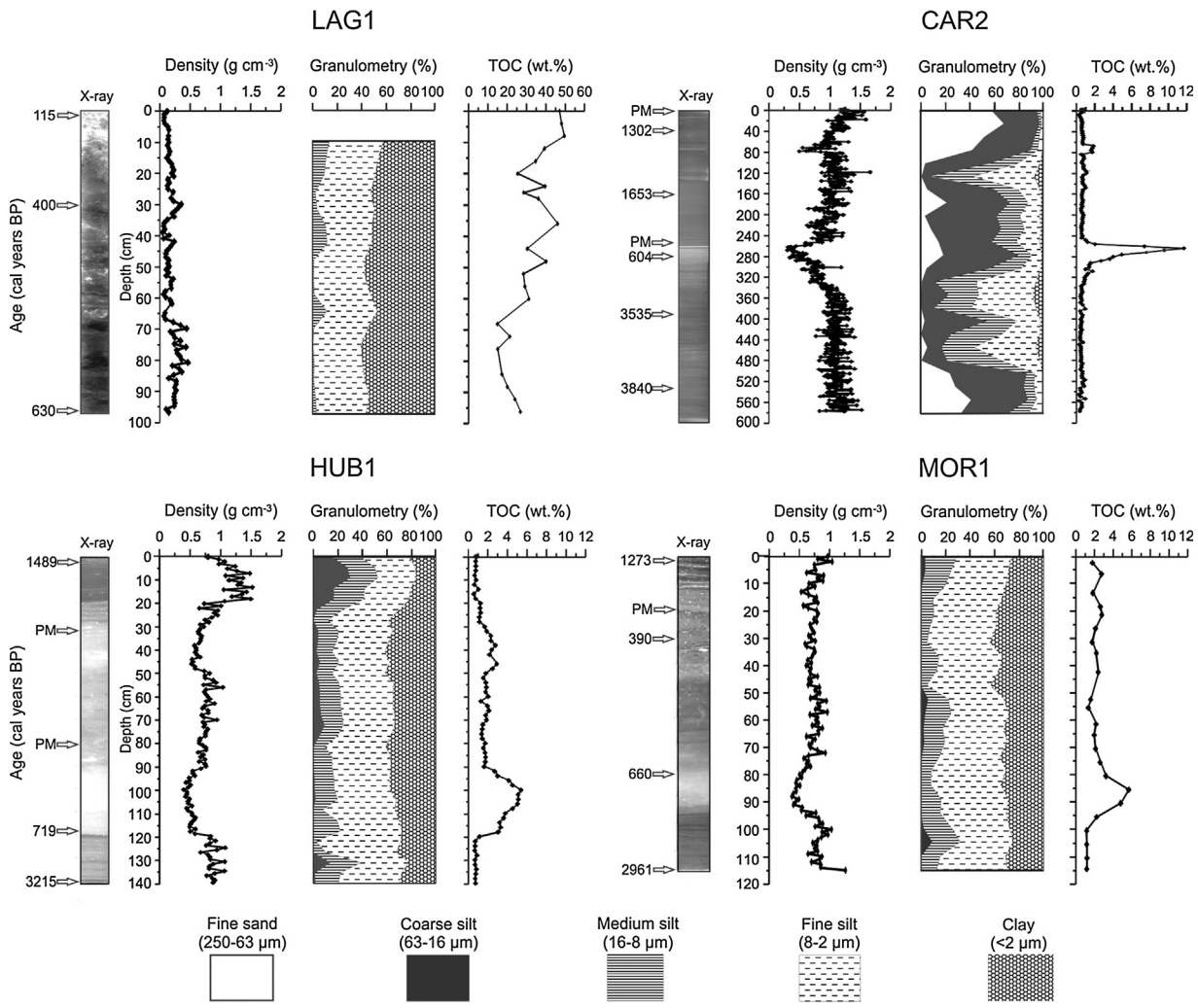

Fig. 3. ^{14}C data, X-ray images, density, particle size analysis, and total organic carbon for the four studied cores.

sediments are transported each year in the upstream part of the Amazon River (Filizola and Guyot, 2009; Filizola et al., 2011; Gibbs, 1967; Guyot et al., 2007; Martinez et al., 2009; Meade et al., 1979). The transport and deposition of this large amount of sediment significantly influences the fluvial dynamics of the Amazonian rivers (Constantine et al., 2014). Historical geomorphological data from the Maranon and Ucayali rivers show that the confluence of the two rivers has migrated from SW to NE during the last century (Dumont, 1996). There are few studies dedicated to the recent dynamics of the Ucayali and Marañón Rivers (Dumont, 1994; Quintana, 2015). Through the study of LANDSAT images, Quintana (2015) estimated an average lateral migration of 140 $m \cdot yr^{-1}$ for the Ucayali River, reaching a peak of 2500 $m \cdot yr-^{1}$ between 1975 and 2011. In contrast, the Marañón River presented a low migration rate during this period, as shown in Fig. 4. Changes in climate and environmental conditions may trigger a range of alterations in the fluvial system (May et al., 2015).

4.2. Late Holocene deposition

During the late Holocene, sedimentation in the Ucayali and Marañón floodplain lakes was characterized by different depositional processes. The chronological models obtained from the three sediment cores collected in the Ucayali floodplain lakes show that sedimentation was not gradual and continuous. The CAR2 core, from Lake Carmen, is the only one with expressive sandy sedimentation, mainly at its base and its top, indicating stronger hydrodynamics in this lake. The base of the core is characterized by sandy silt (Fig. 3) deposited between cal 5000 and 3540 ± 80 cal yr BP ($0.06\,g \cdot cm^{-2} \cdot yr^{-1}$). At 3540 ± 80 yr BP, a 90-cm sequence of coarsening-up silts (480–390 cm) settled very quickly. A rapid sedimentation event is also observed at 3000 cal yr BP in the HUB1 core from Lake Hubos (Fig. 2), but it does not present a granulometric trend. Periods characterized by abrupt accumulation (i.e. sediment packages of the same age) were also reported for

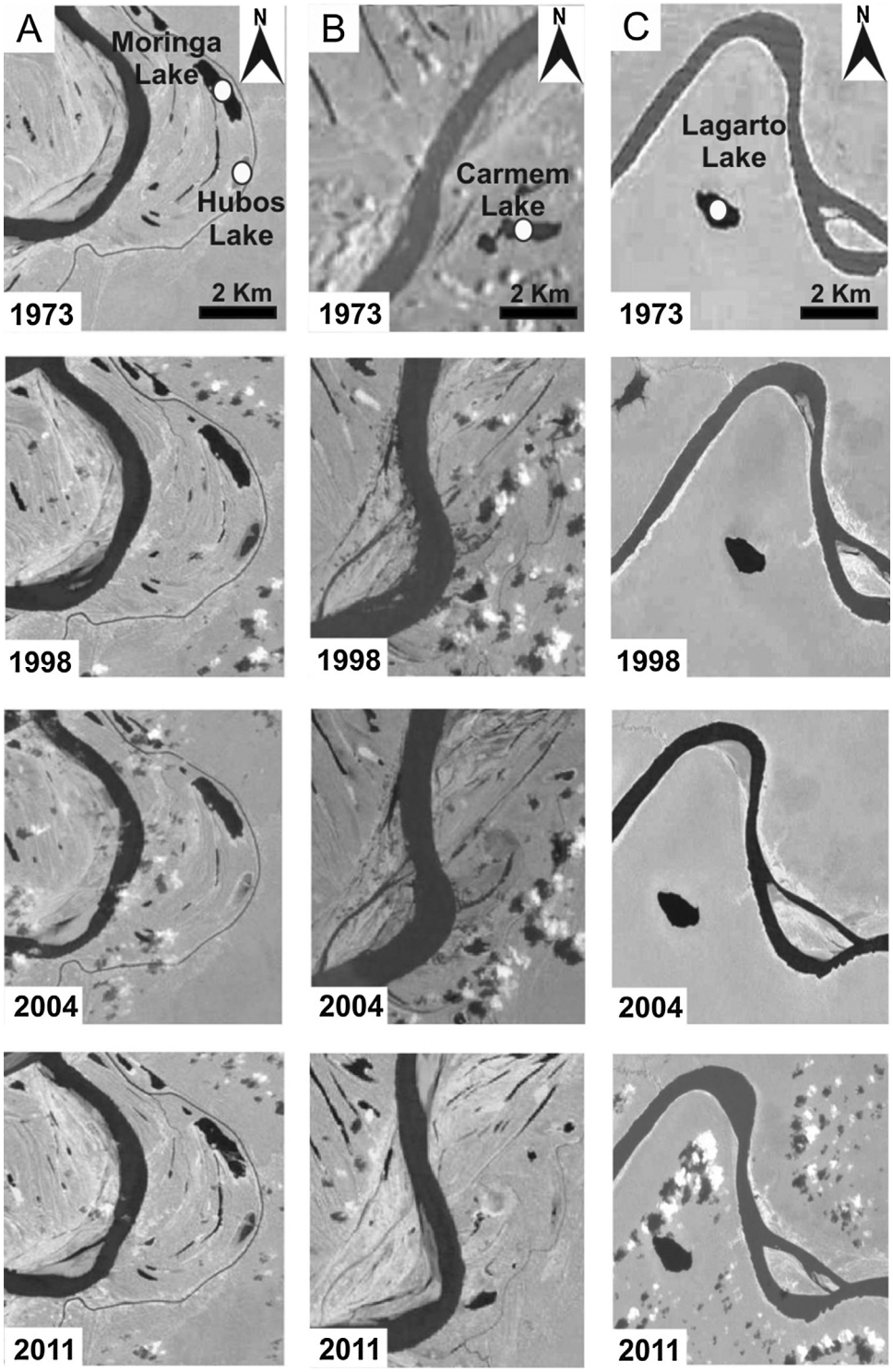

Fig. 4. Temporal evolution of meander migration on the Ucayali and Marañón Rivers floodplains, with core location.

the late Holocene by Moreira-Turcq et al. (2014), and have been interpreted as rapid deposition of sediment packages that probably correspond to one or several successive events of extreme flooding of the Amazon River. This type of deposition by sediment packages has also been evidenced in modern sediments from the Beni floodplain (Aalto et al., 2003), where they correspond to extreme floods associated with La Niña events. The CAR2 480–390-cm and HUB1 140–

120-cm layers also seem to correspond to that kind of sedimentary process, related to overbank deposition and associated with the erosion of inlet channels and levees during very high floods. These flood occurrences are in agreement with a relative humid episode evidenced between 3500 and 2800 cal yr BP in a speleothem from Huagapo Cave, in the central Peruvian Andes (Kanner et al., 2013). After this event, the record of CAR2 shows the deposition of fine silt sediments, with a lower accumulation rate of 0.04 $g \cdot cm^{-2} \cdot yr^{-1}$, while in HUB1 the sedimentation stopped at 3000 cal yr BP. Both reflect a decrease in river sediment supply to the lakes, which may be due to a reduction in river discharge or, more likely, considering the high dynamics of river migration in the Ucayali floodplain (see Fig. 1), a migration of the main river course away from the lakes. The trend of increasing precipitation recorded in the central Andes between ca 6500 and 2500 cal yr BP (Bird et al., 2011; Kanner et al., 2013; Seltzer et al., 2000; Thompson et al., 1995) reinforced the hypothesis of a change in river position rather than a decrease in river discharge. In Lake La Moringa, core MOR1, the accumulation rate is also low (0.013 $g \cdot cm^{-2} \cdot yr^{-1}$) between 2960 and 660 cal yr BP, reflecting a weak influence of the river during this period. At 720 ± 45 cal yr BP, deposition resumed in HUB1 with a rate of 0.03 $g \cdot cm^{-2} \cdot yr^{-1}$, while at 620 ± 60 cal yr BP in MOR1, the accumulation rate increased to 0.09 $g \cdot cm^{-2} \cdot yr^{-1}$, evidencing renewed influence of river supply, culminating with a 15-cm sediment package at 390 cal yr BP. This deposition increase was probably due to the return of the river's main channel to a closer location to Lakes Hubos and La Moringa, until it reached its present-day position.

In contrast, sedimentation in the LAG1 core from Lagarto Lake in the Marañón floodplain is very different, although this core only reached the last 600 cal yr BP. The core is characterized by fine sediments with high TOC values and a rapid constant sedimentation rate of 0.22 $cm \cdot yr^{-1}$ from the base to the top of the core. Hydrodynamics are weaker in that lake, which is surrounded by palms and characterized by low-density sediment, resulting in an accumulation rate between 0.01 to 0.09 $g \cdot cm^{-2} \cdot yr^{-1}$, which is greatly supported by accumulation of organic matter (20% to 50% TOC). Organic sedimentation in Lake Lagarto reflects significant inputs from the local watershed (dominated by *Mauritia flexuosa*) and probably in situ primary production. Lake Quistococha, in the Iquitos region, also presents an organic sedimentation due to *Mauritia flexuosa* and algae production during the last 2600 yr cal BP (Aniceto et al., 2014). We estimated the mean river sediment supply to the lake at about 0.06 $g \cdot cm^{-2} \cdot yr^{-1}$ between 630 and 500 cal yr BP, which however lowered to 0.02 $g \cdot cm^{-2} \cdot yr^{-1}$ after 400 cal yr BP. This decrease in sediment supply may be due to lateral migration of the river's main channel, although there is no evidence of recent meander migrations in that section of the Marañón River (Fig. 1), or to a decrease in river discharge since 600 cal yr BP. The analysis of Landsat images confirms the relative stability of the Marañón meanders (Dumont, 1996; Quintana, 2015). Lower precipitation is observed in the Andes since 1600 AD (Apaéstegui et al., 2014; Bird et al., 2011; Kanner et al., 2013; Thompson et al., 1995) and would explain the reduced discharge of the Marañón River during that period.

4.3. Extreme events deposition

Channel migration is a natural process that remobilizes old alluvial sediments, which mix with modern sediments transported by the river from actively eroding hill slopes (Wittmann et al., 2011). Our data show that sediment stratigraphy in Ucayali floodplain lakes over the past 4000 years is characterized by the presence of packages of very high sedimentation rates (abrupt accumulation) in the three Ucayali cores (Fig. 2). The very short duration of this deposition is below the ^{14}C resolution, and the age of these packages varies between 400 and 3500 cal yr BP. These packages are interpreted as the rapid deposition of sediment that probably corresponds to one or several successive events of extreme flooding of the Ucayali River (Moreira-Turcq et al., 2014). These are characterized by the presence of older ^{14}C age values in the sediment layer, which are interpreted as a contribution of older reworked alluvium. We also observed reworked sediments in the top unit of the Ucayali floodplain cores (Fig. 2), whose ages vary between 600 and 2800 yr BP, deposited upon lake sediment younger than 1950 AD (post-bomb). These sediment packages have a thickness of 250, 30, and 15 cm in Lakes Carmen, Hubos, and La Moringa, respectively. These packages were thicker in the lake nearest the river main channel, as observed in the Carmen sedimentary records. They record a modern period of very high floods that reworked past alluvial sediments of the Ucayali floodplain.

In the case of Lake Carmen, this modern deposition is directly linked to the invasion of the lake by a meander of the Ucayali River (Fig. 4). Due to lateral meander migration, the river levee migrated into Carmen Lake and rebuilt itself over past lacustrine deposits. Based on several satellite images (Fig. 4), we can determine that, in 2004, the river levee reached the lake and cut almost half of its surface. In the case of Lakes La Moringa and Hubos, however, the river remains farther away, and the modern deposition of reworked sediments implies an occurrence of extreme flooding during the past 60 years, at most.

Extreme hydroclimatic events can multiply the effects of the natural channel migration process, and Carmen Lake modern deposition, related to meander migration, may also be a consequence of an increase in flood magnitude. This migration began in 1989, after a stability of several millennia. The river had migrated to the south 3500 years ago, leaving the proximity of Lake Carmen, but never went north of its position of 1973, as shown by the pattern of older paleochannels on the left bank of the river (Fig. 4). If the resumption of meander migration is linked to the extreme floods registered in Lakes Hubos and La Moringa, it means that these extreme events occurred after 1989. Based on hydrography data, Espinoza et al. (2012) have shown an increase in flood levels in Amazonian rivers after 1980, probably due to current anthropic-driven climate change. Our data confirm that floods from the last 60 years, and probably from the last decade (Espinoza et al., 2009, 2011, 2012), have had a higher impact, in term

of alluvial sediment reworking, than any other floods in the past 3000 years.

5. Conclusion

The change in sedimentation of floodplain lakes near the Marañón and Ucayali River confluence during the late Holocene may be related to the combined effects of geomorphological fluvial processes of channel migration and palaeoclimatic changes during the late Holocene. The sediment accumulation rate appears to be a good proxy for river supply for these lakes, which have a limited watershed. The lower deposition rate in Ucayali floodplain lakes since 3540 cal yr BP is interpreted as being related to the changing course of the Ucayali River, which affected the three Ucayali lakes. Events of rapid sediment deposition at 3000 and 3540 cal yr BP, however, reflect extreme floods that occurred during a period of higher precipitation in the central Andes. In the Marañón River Lake, the decrease of river influence since 400 cal yr BP corresponds well with the decrease in precipitation in the Andes.

The modern deposition of reworked sediments, observed in the three Ucayali floodplain lakes, indicates a resumption of meander migration and a strengthening of extreme floods that could be related to present-day climate change.

Acknowledgments

This research was supported by the French Research Institute for Development (IRD) through the SO-Hybam Research Program's cooperation agreement with the Federal Fluminense University (UFF), Brazil. This study was also supported by the INSU Paleo2–PASCAL project (Past Climate Change Impacts on Carbon Accumulation in Amazonia Floodplain Lakes (2010–2012)). The authors would like to thank the technical groups of IRD (ALYSES, Bondy) for their help during the laboratory work. We also thank the SENAMHI-Iquitos group for assistance during core collection. I. Quintana's work is supported by a fellowship from CAPES, Brazil.

References

Aalto, R., Maurice-Bourgoin, L., Dunne, T., Montgomery, D.R., Nittrouer, C.A., Guyot, J.-L., 2003. Episodic sediment accumulation on Amazonian flood plains influenced by El Nino/Southern Oscillation. Nature 425 (6957), 493–497.

Aniceto, K., Moreira-Turcq, P., Cordeiro, R.C., Fraizy, P., Quintana, I., Turcq, B., 2014. Holocene paleohydrology of Quistococha Lake (Peru) in the upper Amazon Basin. Influence on carbon accumulation. Palaeogeogr. Palaeoclimatol. Palaeoecol. 415, 165–174.

Apaéstegui, J., Cruz, F.W., Sifeddine, A., Vuille, M., Espinoza, J.-C., Guyot, J.-L., Edwards, L., 2014. Hydroclimate variability of the northwestern Amazon Basin near the Andean foothills of Peru related to the South American Monsoon System during the last 1600 years. Climate Past 10 (6), 1967–1981.

Armijos, E., Crave, A., Vauchel, P., Fraizy, P., Santini, W., Moquet, J.S., Guyot, J.-L., 2013. Suspended sediment dynamics in the Amazon River of Peru. J. South Am. Earth Sci. 44, 75–84.

Bird, B.W., Abbott, M.B., Vuille, M., Rodbell, D.T., Stansell, N.D., Rosenmeier, M.F., 2011. A 2300-year-long annually resolved record of the South American summer monsoon from the Peruvian Andes. Proc. Natl. Acad. Sci. 108 (21), 8583–8588.

Blaauw, M., 2010. Methods and code for 'classical' age-modelling of radiocarbon sequences. Quat. Geochronol. 5, 512–518.

Constantine, J.A., Dunne, T., Ahmed, J., Legleiter, C., Lazarus, E.D., 2014. Sediment supply as a driver of river meandering and floodplain evolution in the Amazon Basin. Nat. Geosci. 7 (12), 899–903.

Costa, J.B.S., Bemerguy, R.L., Hasui, Y., da Silva Borges, M., 2001. Tectonics and paleogeography along the Amazon River. J. South Am. Earth Sci 14 (4), 335–347.

Dumont, J.-F., Fournier, M., 1994. Geodynamic environment of Quaternary morphostructures of the subandean foreland basins of Peru and Bolivia: characteristics and study methods. Quat. Internat. 21, 129–142.

Dumont, J.-F., 1994. Neotectonics of the Amazon headwaters. In: Schumm, S.A., Winkley, B.R. (Eds.), The variability of large alluvial rivers. ASCE, New York, pp. 103–113.

Dumont, J.-F., 1996. Neotectonics of the Subandes-Brazilian craton boundary using geomorphological data: the Marañón and Beni basins. Tectonophysics 257, 137–151.

Dunne, T., Mertes, L.A., Meade, R.H., Richey, J.E., Forsberg, B.R., 1998. Exchanges of sediment between the flood plain and channel of the Amazon River in Brazil. GSA Bull. 110 (4), 450–467.

Espinoza, J.C., Guyot, J.-L., Ronchail, J., Cochonneau, G., Filizola, N., Fraizy, P., Vauchel, P., 2009. Contrasting regional discharge evolutions in the Amazon basin (1974–2004). J. Hydrol. 375 (3), 297–311.

Espinoza, J.C., Ronchail, J., Guyot, J.-L., Junquas, C., Vauchel, P., Lavado, W., Pombosa, R., 2011. Climate variability and extreme drought in the upper Solimões River (western Amazon Basin): understanding the exceptional 2010 drought. Geophys. Res. Lett. 38 (13.) .

Espinoza, J.C., Ronchail, J., Guyot, J.-L., Junquas, C., Drapeau, G., Martinez, J.-M., Espinoza-Villar, R., 2012. From drought to flooding: understanding the abrupt 2010–2011 hydrological annual cycle in the Amazonas River and tributaries. Environ. Res. Lett. 7 (2), 024008.

Espinoza-Villar, R.E., Martinez, J.-M., Guyot, J.-L., Fraizy, P., Armijos, E., Crave, A., Lavado, W., 2012. The integration of field measurements and satellite observations to determine river solid loads in poorly monitored basins. J. Hydrol. 444, 221–228.

Filizola, N., Guyot, J.-L., 2009. Suspended sediment yields in the Amazon bassin: an assessment using the Brazilian national data set. Hydrol. Processes 23 (22), 3207–3215.

Filizola, N., Guyot, J.-L., Wittmann, H., Martinez, J.-M., Oliveira, E., 2011. The significance of suspended sediment transport determination on the Amazonian hydrological scenario. In: Manning, D.A. (Ed.), Sediment transport in aquatic environments. InTech (332 p.).

Franzinelli, E., Igreja, H., 2002. Modern sedimentation in the lower Negro River, Amazonas State, Brazil. Geomorphology 44 (3), 259–271.

Gibbs, R.J., 1967. Amazon River: environmental factors that control its dissolved and suspended load. Science 156 (3783), 1734–1737 (Remote Sens. 23 (8) 1639–61).

Goulding, M., Barthem, R., Ferreira, E., 2003. The Smithsonian Atlas of the Amazon. Smithsonian Institution Press, Washington D.C (253 p.).

Guyot, J.-L., Bazan, H., Fraizy, P., Ordonez, J.J., Armijos, E., Laraque, A., 2007. Suspended sediment yields in the Amazon basin of Peru: a first estimation. IAHS publication.

Irion, G., Bush, M.B., Nunes de Mello, J.A., Stüben, D., Neumann, T., Müller, G., Morais de, J.O., Junk, J.W., 2006. A multiproxy palaeoecological record of Holocene lake sediments from the Rio Tapajós, eastern Amazonia. Palaeogeogr. Palaeoclimatol. Palaeoecol. 240, 523–535.

Jerolmack, D.J., Mohrig, D., 2007. Conditions for branching in depositional rivers. Geology 35 (5), 463–466.

Kanner, L.C., Burns, S.J., Cheng, H., Edwards, R.L., Vuille, M., 2013. High-resolution variability of the South American summer monsoon over the last seven millennia: insights from a speleothem record from the central Peruvian Andes. Quat. Sci. Rev. 75, 1–10.

Latrubesse, E.M., Franzinelli, E., 2002. The Holocene alluvial plain of the middle Amazon River, Brazil. Geomorphology 44 (3), 241–257.

Marengo, J.A., Tomasella, J., Uvo, C.R., 1998. Trends in streamflow and rainfall in tropical South America: Amazonia, eastern Brazil, and northwestern Peru. J. Geophys. Res. Atmospheres 103 (D2), 1775–1783.

Martinez, J.-M., Guyot, J.-L., Filizola, N., Sondag, F., 2009. Increase in suspended sediment discharge of the Amazon River assessed by monitoring network and satellite data. Catena 79 (3), 257–264.

May, J.H., Plotzki, A., Rodrigues, L., Preusser, F., Veit, H., 2015. Holocene floodplain soils along the Río Mamoré, northern Bolivia, and their implications for understanding inundation and depositional patterns in seasonal wetland settings. Sediment. Geol. 330, 74–89.

Meade, R.H., Nordin, C.F., Curtis, W.F., Rodrigues, F.M.C., Do Vale, C.M., Edmond, J.M., 1979. Sediment loads in the Amazon River. Nature 278 (5700), 161–163.

Meade, R.H., Dunne, T., Richey, J.E., Santos, U.D.M., Salati, E., 1985. Storage and remobilization of suspended sediment in the lower Amazon River of Brazil. Science 228 (4698), 488–490.

Mertes, L.A., Dunne, T., Martinelli, L.A., 1996. Channel-floodplain geomorphology along the Solimões-Amazon river, Brazil. GSA Bull. 108 (9), 1089–1107.
Migeon, S., Weber, O., Faugères, J.-C., Saint-Paul, J., 1998. SCOPIX: a new X-ray imaging system for core analysis. Geomarine Lett. 18 (3), 251–255.
Moreira-Turcq, P., Turcq, B., Moreira, L.S., Amorim, M., Cordeiro, R.C., Guyot, J.-L., 2014. A 2700 cal yr BP extreme flood event revealed by sediment accumulation Amazon floodplains. Palaeogeogr. Palaeoclimatol. Palaeoecol. 415, 175–182.
Quintana, I., 2015. Dinámica de meandros en el Alto Amazonas (Ucayali Basin). Universidad de Cantabria (PhD Thesis, 367 p.)http://www.hdl.handle.net/10902/8110.
Räsänen, M.E., Salo, J.S., Jungnert, H., Pittman, L.R., 1990. Evolution of the western Amazon lowland relief: impact of Andean foreland dynamics. Terra Nova 2 (4), 320–332.
Santini, W., Martinez, J.-M., Espinoza Vilar, R., Guyot, J.-L., Cochonneau, G., Vauchel, P., Moquet, J.S., Baby, P., Espinoza, J.C., Lavado, W., Carrranza, J., Guyot, J.-L., 2014. In book: Sediment Dynamics from the Summit to the Sea, 367. IAHS, 320–325.
Seltzer, G., Rodbell, D., Burns, S., 2000. Isotopic evidence for late Quaternary climatic change in tropical South America. Geology 28 (1), 35–38.
Thompson, L.G., Mosley-Thompson, E., Davis, M.E., Lin, P.N., Henderson, K.A., Cole-Dai, J., Liu, K.B., 1995. Late glacial stage and Holocene tropical ice core records from Huascaran, Peru. Science 269 (5220), 46–50.
Wittmann, H., Von Blanckenburg, F., Maurice, L., Guyot, J.-L., Kubik, P.W., 2011. Recycling of Amazon floodplain sediment quantified by cosmogenic ^{26}Al and ^{10}Be. Geology 39 (5), 467–470.